

# In-Situ Electrospinning Dressings Loaded with Kaempferol for Reducing MMP9 to Promote Diabetic Ulcer Healing

Jianwen Li<sup>1,2,\*</sup>, Hongqi Meng<sup>3,\*</sup>, Wenlai Guo<sup>3</sup>, Lubin Zhou<sup>4</sup>, Siyu Wu<sup>3</sup>, Guanghui Gao<sup>4</sup>, Quanzhe Liu<sup>3</sup>, Di You<sup>5</sup>, Wenrui Qu<sup>2,3</sup>

<sup>1</sup>Gastroenteric Medicine and Digestive Endoscopy Center, the Second Hospital of Jilin University, Changchun, 130041, People's Republic of China; <sup>2</sup>Joint International Research Laboratory of Ageing Active Strategy and Bionic Health in Northeast Asia of Ministry of Education, Changchun, 130041, People's Republic of China; <sup>3</sup>Department of Hand Surgery, the Second Hospital of Jilin University, Changchun, 130041, People's Republic of China; <sup>4</sup>Polymeric and Soft Materials Laboratory, Advanced Institute of Materials Science, School of Chemical Engineering, Changchun University of Technology, Changchun, 130012, People's Republic of China; <sup>5</sup>Department of Anesthesiology, China-Japan Union Hospital of Jilin University, Changchun, 130012, People's Republic of China

\*These authors contributed equally to this work

Correspondence: Di You; Guanghui Gao, Email youdi1118@jlu.edu.cn; ghgao@ccut.edu.cn

**Background:** Diabetic foot ulcers (DFUs) are often associated with persistent inflammatory response, impaired macrophage polarization, and slow vascular regeneration. Existing treatments cannot be adapted to wounds and do not achieve the desired therapeutic effects. The high porosity of biomaterials induces more M2 macrophages, while the natural compound kaempferol inhibits the expression of matrix metalloproteinase 9 (MMP9) and thus inhibits the associated inflammatory and immunological responses.

**Methods:** portable electrospinning dressings (PEDs) were prepared from the spinning solution using a portable electrospinning device. The material properties of PEDs were examined by scanning electron microscope, contact angle tester and WVTR-C3. Then, the in vitro biocompatibility of the dressings was evaluated using NIH3T3 cells. The in vivo wound healing efficacy of the dressings was analyzed in the diabetic wound model rats. Histological and immunofluorescence staining were performed to determine the status of epithelization, collagen deposition, MMP9 expression, macrophage polarization, inflammation response and angiogenesis.

**Results:** Material science experiments have shown that the dressing has optimal fiber micromorphology and good water vapor transport properties (WVTR:  $4.88 \text{ kg m}^{-2} 24\text{h}^{-1}$ ); in vivo, diabetic wound experiments have shown that the high porosity and pharmacological effects of PED4 can mutually promote the rapid healing of diabetic wounds (healed 95.9% on day 15), facilitate the transformation of macrophages from M1-type to M2-type and regulate the expression of MMP9.

**Conclusion:** Portable electrospinning dressings equipped with kaempferol not only better fit irregular wounds, but also promote wound healing through MMP9 and macrophage polarization. Thus, PEDs show great promise for advancing research of personalized diabetic wound healing.

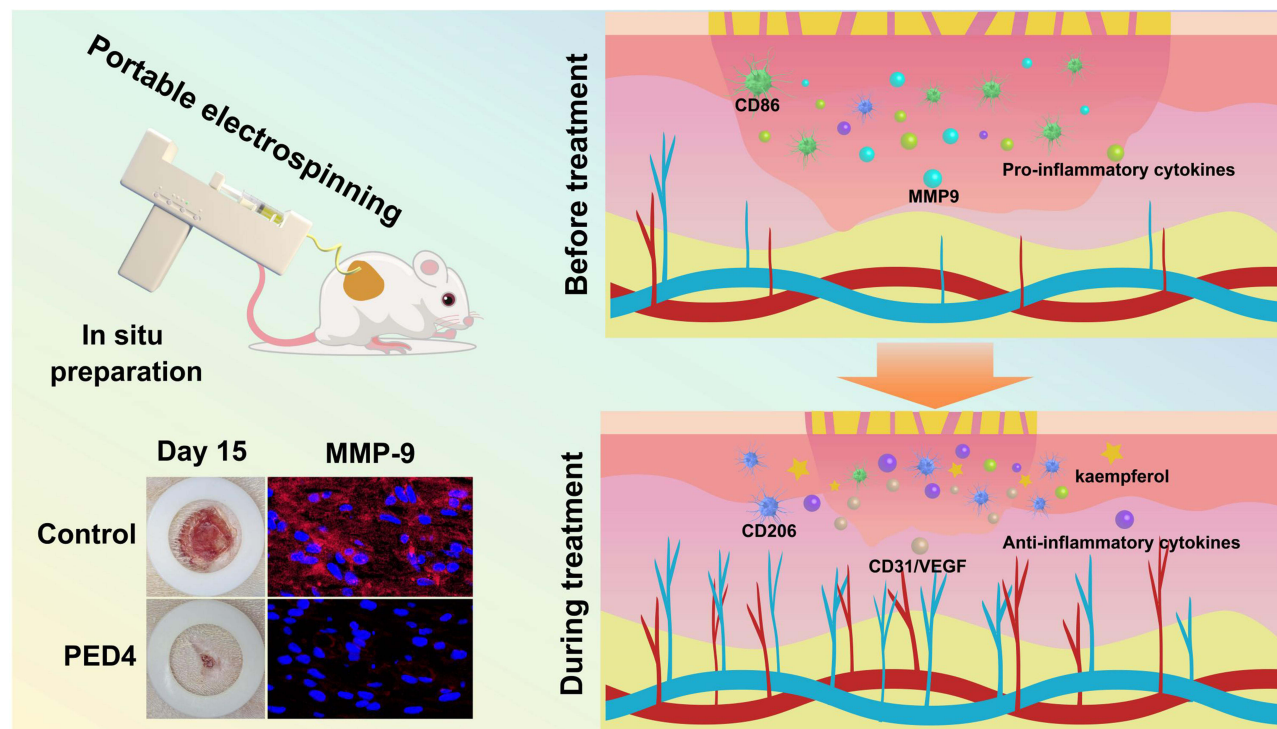
**Keywords:** portable electrospinning, kaempferol, MMP9, macrophage immunomodulation, inflammatory exudate, neovascularization

## Introduction

Diabetic foot ulcers (DFUs) impact 19%–34% of the estimated 537 million individuals with diabetes worldwide.<sup>1</sup> DFUs are known to cause long-term pain, impair movement, significantly reduce the quality of life, and impose a substantial psychological load.<sup>2</sup> The economic toll of treating DFUs has been estimated to range between \$9 billion and \$13 billion annually, thus presenting a significant financial burden.<sup>3</sup> The conventional approach for treating DFUs involves wound debridement with antibiotics to address infections, but this method is often ineffective.<sup>2</sup> The ineffectiveness of the treatment may stem from immunomodulatory dysfunction in patients with diabetes, leading to diminished conversion of the macrophage M1 phenotype to the M2 phenotype or the over-polarization of M1 macrophages.<sup>4,5</sup> Additionally, it



## Graphical Abstract



could be associated with elevated activity levels of some matrix metalloproteinases (MMPs), with heightened Matrix Metalloproteinase-9 (MMP9) expression hindering proper extracellular matrix (ECM) formation and slowing down the transition from the proliferative phase of the wound to the remodeling phase.<sup>6,7</sup> The collective impact of these factors results in an extended inflammatory duration in diabetic wounds, an overabundance of inflammatory factors like tumor necrosis factor- $\alpha$  (TNF- $\alpha$ ), interleukin (IL)-1 $\beta$ , and IL-6, diminished collagen deposition, and reduced neovascularization.<sup>8,9</sup> In the clinical application of DFU therapy, traditional dressings such as gauze and cotton mainly cover and protect wounds, resulting in the inability to achieve the desired therapeutic clinical outcomes of DFUs. Consequently, developing novel dressings to achieve effective DFU treatment is urgently needed.

Recently, various biomaterials have been developed for treating chronic wounds, including sponges,<sup>10</sup> hydrogels,<sup>11</sup> nanoparticles,<sup>12</sup> and others. Electrostatic spinning, which involves electrostatic forces to create fibrous membranes from polymer solutions or molten states, has emerged as a promising approach. This technique produces a fibrous membrane with high porosity and good pore interconnectivity, which creates a microenvironment conducive to cellular response and wound healing, inducing more M2 macrophages.<sup>13,14</sup> Portable electrospinning filaments, a novel electrospinning filament variant, can rapidly produce films with strong adhesion to uneven tissues. Portable electrospinning devices are lightweight and portable, allowing personalized dressing preparation tailored to specific wounds.<sup>15–17</sup> The efficient natural drug loading capability of electrospinning dressings has garnered significant attention in wound dressing research.<sup>18</sup> For instance, Zhou et al prepared a self-pumping dressing incorporating gastadin through double-layer electrospinning to alleviate inflammation by draining wound exudates.<sup>19</sup> Yue et al developed a multifunctional portable electrostatic spinning device to directly apply antimicrobial fiber membranes with suitable breathability and mechanical properties to the human skin.<sup>20</sup> Similarly, Zhao et al utilized a portable melt electrospinning device to expediently generate nanofiber membranes, such as those made from polycaprolactone, on wound surfaces.<sup>21</sup> However, these studies have



limitations, including the absence of *in vivo* experiments to assess therapeutic efficacy, potential risks of burns to the wound or surrounding skin, and the complexity and lengthiness of dressing preparation procedures.

This study, kaempferol was selected as a natural compound component of the dressing. Kaempferol is a naturally occurring flavonoid recognized for its positive effects on human health, including anti-inflammatory, antioxidant, anti-diabetic, and atherosclerotic properties.<sup>22–24</sup> Prior studies have demonstrated that kaempferol could reduce MMP9 activity and protein levels by modulating signaling pathways, facilitating macrophage phenotype polarization, and decreasing proinflammatory cytokine expression.<sup>25–27</sup> Moreover, kaempferol inhibits the Mitogen-activated protein kinases (MAPKs)/ nuclear factor- $\kappa$ B (NF- $\kappa$ B) signaling pathway, suppresses the production of inflammatory factors such as IL-1 $\beta$ , and effectively alleviates the intensity of inflammatory response.<sup>28</sup> Therefore, we used portable electrospinning technology loaded with kaempferol to design dressings that can be used for individualized and timely treatment of irregular wounds.

Based on the above theory, we designed a portable electrospinning dressing (PED) and a PED loaded with kaempferol (PED4) (Scheme 1). PED4 integrates physical barriers against external microorganisms, promotes macrophage polarization, inhibits MMP9 expression, and reduces the expression of inflammatory factors. When interacting with diabetic wounds, PED4 enhanced the inhibitory action of kaempferol on MMP9 and simultaneously directed the immunomodulatory response of macrophages, promoting their M1 to the M2 phenotype transition. This regulation of the inflammatory response in DFUs facilitated vascular regeneration. The effectiveness of PED4 in wound treatment was validated in a diabetic rat wound model. Immunostaining analysis confirmed its ability to regulate MMP9, modulate macrophages, and promote neovascularization.

## Materials and Methods

### Materials

Polyvinyl butyral (PVB, Mowital<sup>®</sup> B75H) was procured from Kuraray (Tokyo, Japan). Pluronic F-127 (PF-127) was obtained from Sigma Aldrich (Shanghai, China). Ethanol (AR, 99.98%) was obtained from Guanghua Sci-Tech (Guangdong, China). Kaempferol was bought from Macklin (Shanghai, China). BacLight LIVE/DEAD cell viability kits were obtained from Molecular Probes (Eugene, Oregon, USA). Primary antibodies for TNF- $\alpha$ , IL-1 $\beta$ , IL-6, and IL-10, cluster of differentiation 31 (CD31), and vascular endothelial growth factor (VEGF) were procured from BIOCSS BioTech Co. Ltd (Beijing, China). NIH/3T3 cells were provided by Solarbio Ltd. (Beijing, China).

### Preparation of the PED

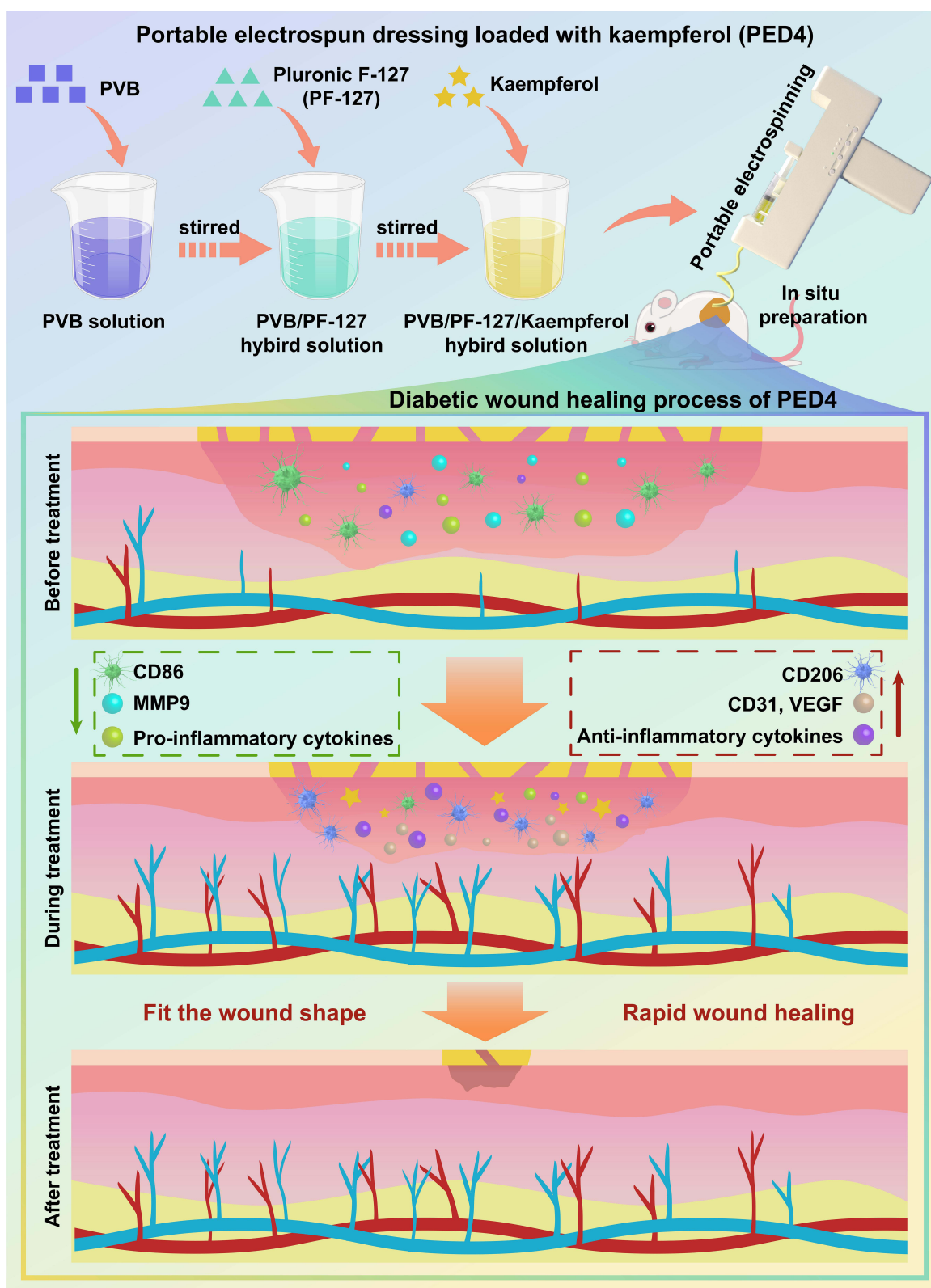
First, 5% (w/v) PVB, 1% (w/v) kaempferol, and varying concentrations of PF-127 (0, 10%, 15%, and 20% (w/v)) were dissolved in ethanol and stirred uniformly to obtain four spinning solutions. The PED was prepared from the above-mixed spinning solution using portable electrospinning equipment (HED-03, Huizhi Electric spinning, China). The specific parameters were as follows: 2 mL of mixed spinning solution; 21 G needle; DC voltage: 15 kV; spinning distance: 10–15 cm; propulsion speed: 10 mL h<sup>-1</sup>.

Then, 5% (w/v) PVB, 1% (w/v) kaempferol, and 15% (w/v) PF-127 were dissolved in ethanol and uniformly stirred to obtain a kaempferol spinning solution. PED4 was prepared from the above-mixed spinning solution using portable electrospinning equipment (HED-03, Huizhi Electric spinning, China). The specific parameters were as follows: 2 mL of spinning solution; 21 G needle; DC voltage: 15 kV; spinning distance: 10–15 cm; propulsion speed: 10 mL h<sup>-1</sup>. The abbreviations for PED are demonstrated in Table 1.

### Characterization

The surface characteristics of the PED dressings were examined using scanning electron microscopy (SEM; Phenom Pro, Thermo Fisher Scientific, USA). The dynamic wettability of the PED dressings was evaluated using a contact angle tester (DSA30, KRÜSS, Germany). The 150 mg of PED2 and PED4 fiber membranes were weighed, and each sample was immersed in 25 mL of PBS buffer solution (PH = 7.2–7.4). The suspension was stored in a 37 °C water bath for 6 h. 3.0 mL of solution was taken out from the dissolution medium, and the absorbance was detected by a UV-visible





**Scheme 1** Preparation method and schematic diagram of the action of PED4. PED4 contains PVB, PF-127, and kaempferol. PED4 inhibits MMP9 expression and promotes macrophage polarization.



**Table 1** Abbreviation for PED with Different Contents of PF-127

Portable Electrospinning Dressing (PED)			Abbreviations
PVB	Kaempferol	PF-127	
5%	0%	0%	PED0
5%	0%	10%	PED1
5%	0%	15%	PED2
5%	0%	20%	PED3
5%	1%	15%	PED4

spectrophotometer (UV-1780, SHIMADZU). The water vapor transmission rates (WVTR) of the gauze and PED dressings were tested using a WVTR-C3 (SYSTESTER, China). The temperature was maintained at  $36 \pm 0.5$  °C, while the relative humidity was controlled at  $60\% \pm 1\%$ .<sup>9</sup>

## Cytotoxicity Analysis

The biocompatibility of the dressing was assessed by measuring NIH/3T3 fibroblast proliferation on days 1, 3, and 5 using the Cell Counting Kit-8 (CCK8), and by evaluating cell survival with the live/dead cell staining. NIH/3T3 cells were treated with different materials such as gauze, PED0, PED2, and PED4. On days 1, 3, and 5, the optical density (OD) values at 450 nm were measured. Subsequently, a live/dead staining assay was performed to evaluate the biocompatibility of various materials. Gauze, PED0, PED2, and PED4 were introduced into 24-well culture plates and incubated with NIH/3T3 fibroblasts for 24 hours. Subsequently, the cells were treated with calcein AM and PI working solutions in a dark environment.<sup>19</sup>

## Evaluation of Wound Healing in Rats with Total Skin Defects

Fifteen specific pathogen-free (SPF) male Sprague-Dawley rats were selected for the study. After fasting, rats were induced to establish a type I diabetes model by intraperitoneal injection of streptozotocin (STZ, 50 mg/kg) in sodium citrate solution. Three days later, the non-modeled rats were re-dosed until all rats successfully established the diabetes model. Fifteen type I diabetic rats were randomly divided into five groups: control, gauze, PED0, PED2, and PED4. The control group received no treatment; the remaining groups changed their corresponding dressing every three days. During this procedure, the wounds of diabetic rats in each group were recorded at 0, 3, 6, 9, 12, and 15 days.

Wound residual area (%) =  $[W(0, 3, 6, 9, 12, 15)/W(0)] \times 100\%$ , where  $W(0)$  and  $W(0, 3, 6, 9, 12, 15)$  respectively represent the wound area of diabetic rats on days 0, 3, 6, 9, 12 and 15.<sup>29</sup>

All animal experimentation was performed within an SPF environment. All animal procedures received approval from the Laboratory Animal Ethics Committee at Jilin University (Changchun, China, Approval No. KT202303027). These experiments adhered to the guidelines established by the National Institutes of Health concerning the care and use of experimental animals and complying with international ethical standards.

## Pathological-Histological and Immunofluorescent Staining

On day 15 of the animal experiment, 15 rats were euthanized, and the skin tissues were immediately extracted from the center of the wounds. The tissues were then embedded in paraffin and sliced into sections measuring 5  $\mu$ m in thickness. Then, histological analysis was performed with hematoxylin and eosin (H&E) and Masson trichrome staining (MT). Immunofluorescence staining was performed utilizing different antibodies, and sections were incubated with rabbit anti-rat primary antibodies (MMP9, TNF- $\alpha$ , IL-1 $\beta$ , IL-6, IL-10, CD31, VEGF, CD86, CD206) and goat anti-rabbit secondary antibodies, respectively.<sup>12,30</sup> Finally, fluorescent images captured by confocal microscopy were analyzed and illustrated and analyzed using the ImageJ software.



## Statistical Analysis

The results are expressed as mean  $\pm$  standard deviation ( $n = 3$ ). A single asterisk (\*) represents  $p < 0.05$ , while a double asterisk (\*\*) signifies  $p < 0.01$  compared to the control group. Furthermore,  $P < 0.05$  for gauze/PED0 group comparisons, gauze/PED2 group comparisons, and gauze/PED4 group comparisons are denoted by # (well signs),  $\Delta$  (triangles), and  $\diamond$  (diamonds), respectively.

## Results and Discussion

### Preparation of the PED

To improve the conformability of wound dressings to irregularly shaped wounds, a portable electrospinning device was used to perform in situ electrospinning at the wound site to prepare wound dressings to protect the wound while promoting wound healing. Compared with the traditional desktop electrospinning machine, the portable electrospinning device is small, lightweight, and flexible ([Figure S1](#)). When a portable electrospinning device was used to prepare an electrospinning dressing, the aluminum foil changed from a bright silver color (reflective) before spinning to a white color (non-reflective) after spinning ([Figure 1a](#) and [b](#)). In the electrospinning process, the droplet was stretched into ultrafine nanofibers using a 15 kV DC voltage, followed by rapid solvent evaporation and final deposition on an aluminum foil ([Video S1](#)). Among them, the nanofibers are visible ([Figure 1c](#)).

### Characterization of PED

To evaluate the dynamic apparent contact angle of the PED dressings containing different PF-127 contents, the contact angles of the PED dressings were tested using a contact angle tester. As depicted in [Figure 2a](#), PED0 of pure PVB without PF-127 exhibits hydrophobicity due to the hydrophobicity of PVB and, therefore, does not absorb liquid. When the PF-127 content in the PED was 10% and 15%, the contact angles of PED1 and PED2 exhibited excellent hydrophobicity ([Figure 2b](#) and [c](#)). Although the contact angle of PED1 was reduced to  $0^\circ$  at only 0.64 s, its spinning process kept dripping liquid, leading to poor spinning effects. Its SEM characterization illustrated that most of the fibers were in a state of being dissolved into one ([Figure S2](#)). However, when the PF-127 content of PED3 reached 20%, the contact angle of PED3 slowly decreased. The contact angle of the PED3 dressing reduced from  $61.2^\circ$  to  $46.6^\circ$  in 4.56 s ([Figure 2d](#) and [Video S2](#)). This is because too much PF-127 caused the fibers to become coarser and more wrinkled ([Figure S3](#)), which increased the roughness and density of the fibers; thus, the fibers absorbed liquid very slowly. Therefore, although it took 4.96 s for the water contact angle of PED2 to drop to  $0^\circ$ , the nanofibers in PED2 prepared using the portable electrospinning devices were uniform and displayed optimal morphology ([Figure 3](#) and [Figure S4](#)).

Therefore, kaempferol was added to PED2 to obtain the kaempferol-loaded PED4. The water contact angle of PED4 decreased to  $18.0^\circ$  in 4.96 s, which was an improvement compared to that of PED2, due to the hydrophobic properties of the added kaempferol ([Figure 2e, f](#) and [Video S3](#)). PED4 showed kaempferol UV absorption peaks at wavelengths of 267.8 nm and 371.0 nm, and the rapid release of kaempferol in PED4 turned the solution into yellow ([Figure S5](#)).

WVTR testing exhibited that the WVTR of the gauze group ( $9.40 \text{ kg m}^{-2} 24\text{h}^{-1}$ ) was the highest ([Figure 2g](#)). However, the WVTR of PED2 without kaempferol ( $4.85 \text{ kg m}^{-2} 24\text{h}^{-1}$ ) and PED4 with kaempferol ( $4.88 \text{ kg m}^{-2} 24\text{h}^{-1}$ ) were similar. Thus, adding kaempferol had little effect on WVTR. The WVTR of PED2 and PED4 allowed the

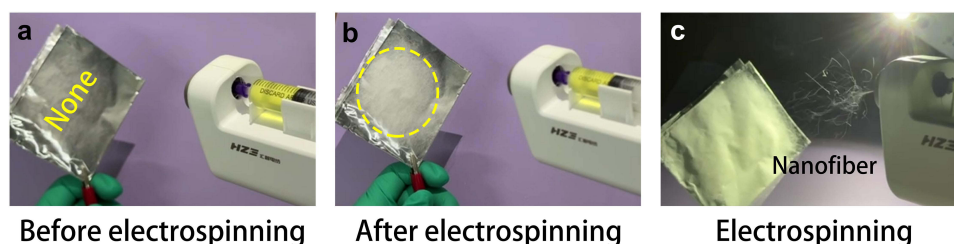


**Figure 1** Process demonstration images of portable electrospinning. (a) State of the aluminum foil before electrospinning. (b) State of aluminum foil after electrospinning. (c) Demonstration of nanofibers during electrospinning.



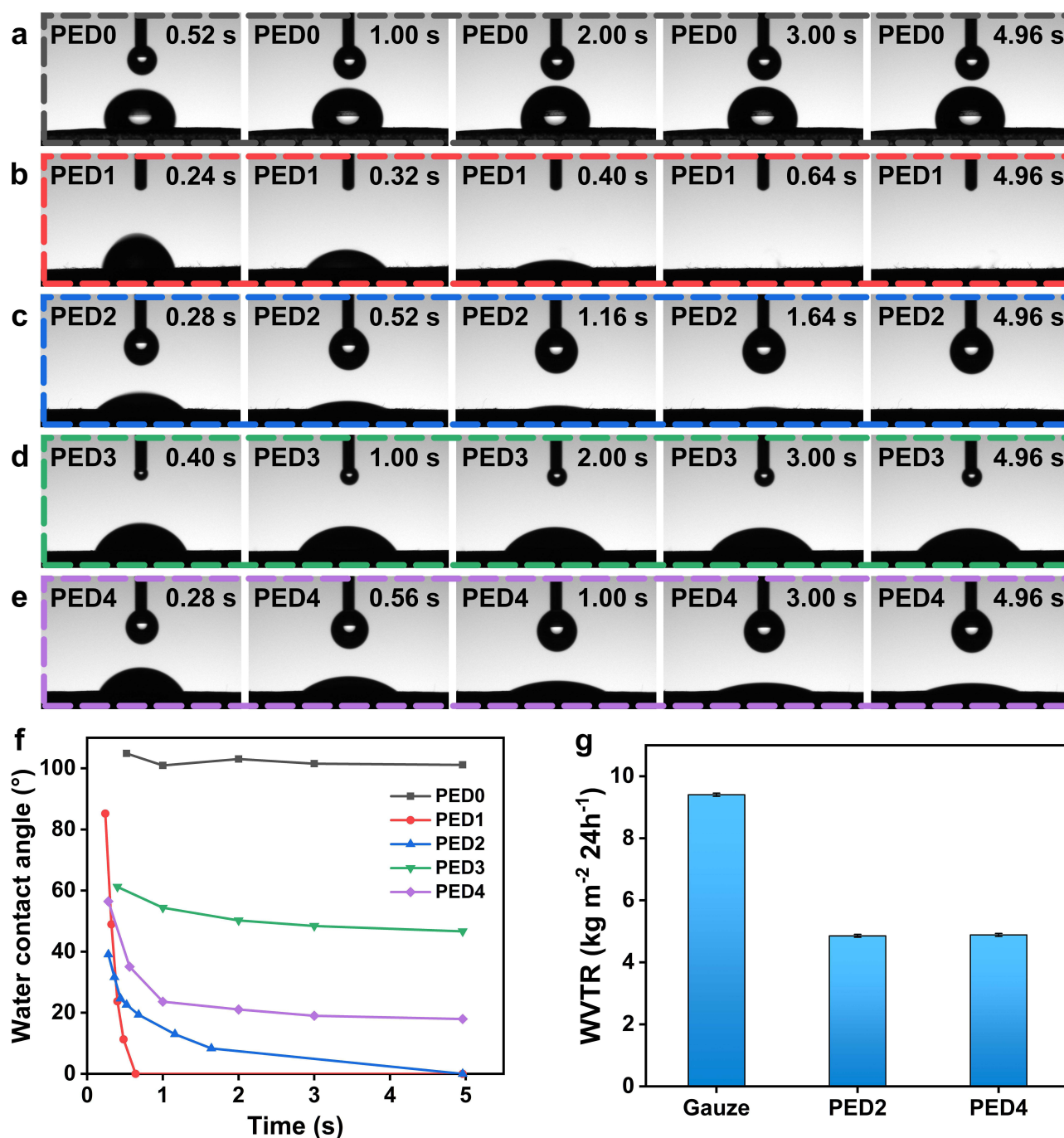


**Figure 2** Characterization of PED dressings with different PF-127 contents. (a–e) Contact angle images of the dynamic variation for PED0 (a), PED1 (b), PED2 (c), PED3 (d), and PED4 (e). (f) Dynamic variation curves of contact angles for PED0, PED1, PED2, PED3, and PED4. (g) WVTR of different dressings.

evaporation and accumulation of wound water to be effectively maintained at a state suitable for wound healing. As a result, PED2 and PED4 possessed excellent water vapor transmission properties.

To further evaluate the effect of varying PF-127 concentrations on the microscopic morphology of portable electrospinning, the fiber diameters of PED0 to PED3 gradually coarsened with increasing PF-127 content. However, the fiber diameter distribution could not be accurately measured because the fibers dissolved together in PED1 and the relatively irregular morphology of the fibers with multiple folds in PED3. The mean fiber diameters of PED2 (2.37  $\mu\text{m}$ ) and PED4 (2.28  $\mu\text{m}$ ) were similar, indicating that the addition of kaempferol had a non-significant influence on the fiber diameter of PED. In short,



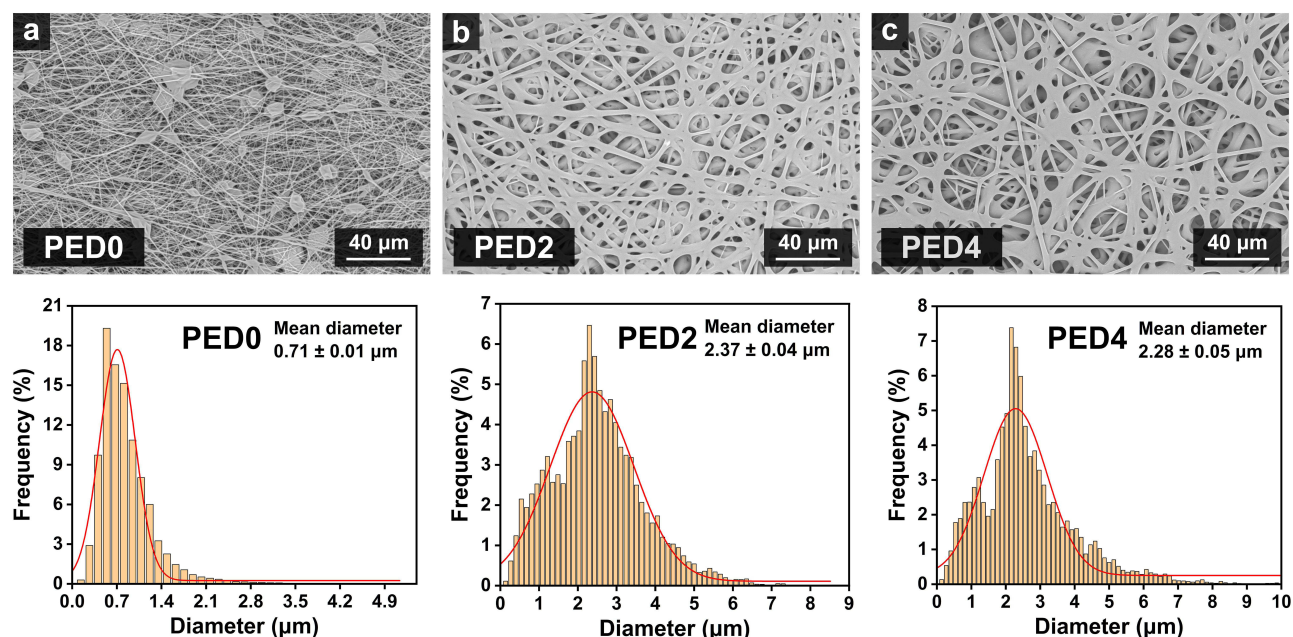


**Figure 3** SEM images and fiber diameter distribution of PED dressings. (a–c) SEM images and fiber diameter distribution of PED0 (a), PED2 (b), and PED4 (c).

PED2 and PED4 exhibited optimal fiber micromorphology when the PF-127 content was 15%. Therefore, PED2 and PED4 were selected for subsequent experiments, including *in vitro* cytocompatibility and *in vivo* wound healing, to compare their diabetic wound healing effects further.

## Cytocompatibility and Cytotoxicity Tests

Excellent biocompatibility is essential for the use of electrospun filaments in biological dressings.<sup>31</sup> To assess the cytocompatibility of various dressing groups (gauze, PED0, PED2, and PED4), we utilized NIH/3T3 fibroblasts, which are typical for tissue healing. In the proliferation assay, after contacting the cells with gauze, PED0, PED2, and PED4 dressings for 1, 3, and 5 days, the OD values of different groups exceeded 90% of those of the control group, suggesting that the electrospun dressings and their components exhibited non-cytotoxicity and excellent biocompatibility (Figure 4). Similarly, the results of the live/dead cell staining experiments depicted that most cells in all electrospun groups maintained their viability (green) and displayed a spindle-shaped morphology, with only a minimal number of dead cells (red) (Figure 4a). These findings support the conclusion that the tested dressings had a non-significant impact on cell proliferation across all groups, confirming their exceptional cytocompatibility for potential application in wound healing.

## Diabetic Wound Healing Assessment and Histological Analysis

To assess the influence of different electrospinning dressings on wound healing *in vivo*, we constructed a model of total skin defects in type I diabetic rats. Optical images and ratios depicting the wound appearance and residual wound bed area were captured at various time points for the control, gauze, PED0, PED2, and PED4 groups (Figure 5a–c). The gauze group exhibited a marginal improvement in therapeutic efficacy compared to the control group. The PED0 group demonstrated efficacy levels similar to gauze, likely due to its reduced water vapor transmission properties. This phenomenon can be attributed to the extended inflammatory phase during the acute stage of wound healing, which leads to the accumulation of inflammatory mediators and disrupts immune responses. Contrarily, the PED2 and PED4 groups demonstrated enhanced therapeutic effects owing to the modulation of the PF-127 ratio in the dressings, thereby improving water vapor transmission. Incorporating kaempferol in the PED4 group resulted in a pronounced healing trajectory across all stages of wound healing, particularly during the initial phase (Figure 5c), which is the same as the



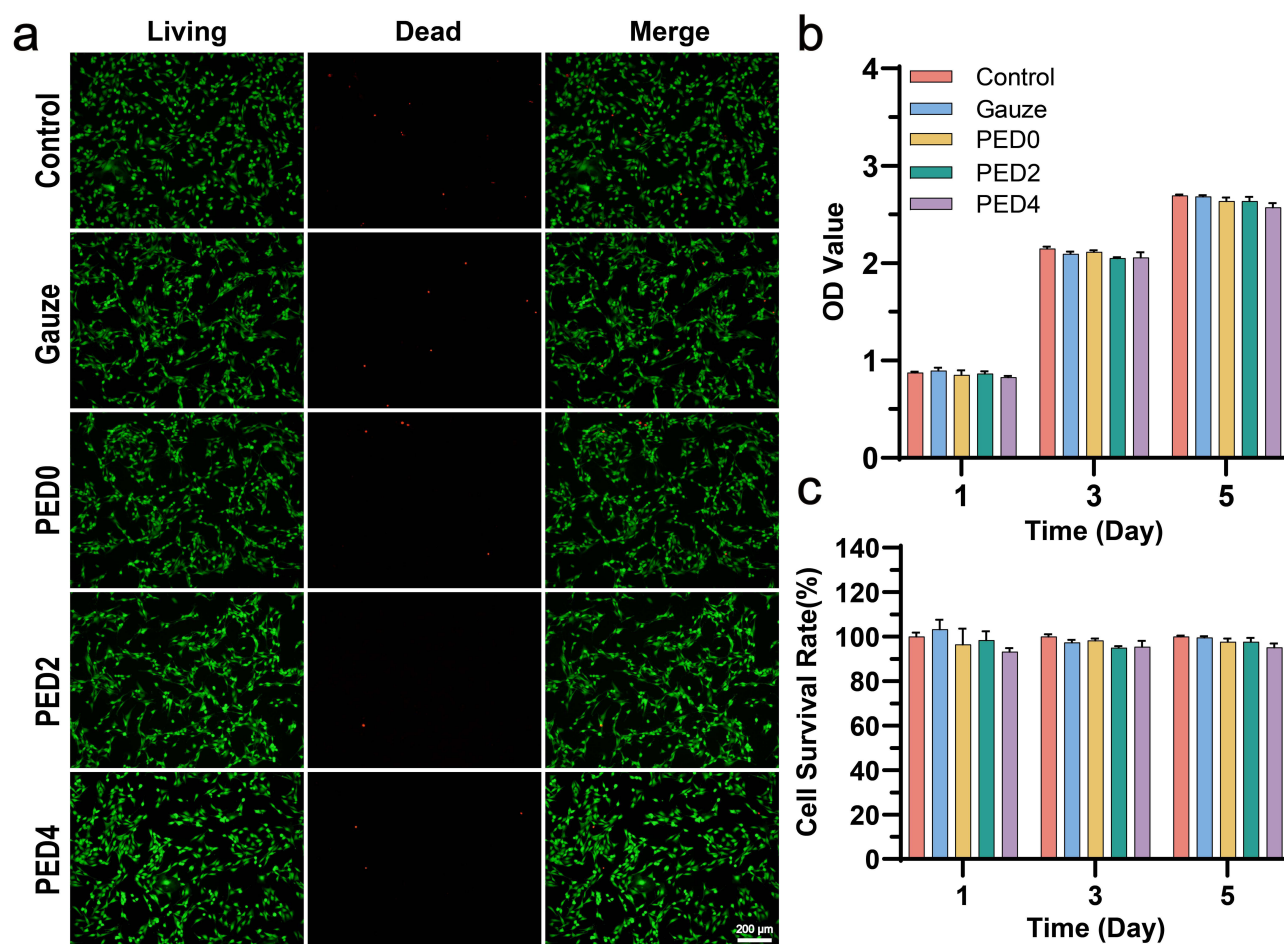


**Figure 4** Effect of different portable electrospun dressings on proliferation and viability of NIH/3T3 cells. (a) Effect of different dressings on viable/dead staining of NIH/3T3 cells. (b) Effect of different dressings on NIH/3T3 cell proliferation ( $n = 3$ ). (c) Analysis of NIH/3T3 cell viability after culture with different dressings ( $n = 3$ ) (\* indicates  $p < 0.05$  compared with the control group; # indicates  $p < 0.05$  compared with PED0 group;  $\Delta$  indicates  $p < 0.05$  compared with PED2 group;  $\diamond$  indicates  $p < 0.05$  compared with PED4 group).

results of a previous study.<sup>32</sup> This enhancement is attributed to the natural flavonol kaempferol, which hinders the NF- $\kappa$ B signaling pathway, suppresses inflammatory factor expression, and influences macrophage polarization.<sup>27,33</sup>

The quality of the regenerated wound tissue was analyzed using H&E and MT staining results (Figure 5d-f). Neither epithelial nor granulation tissue regeneration was evident in the control group, and an unclear trend in wound healing was observed. In contrast, dressing-treated wounds in the PED2 and PED4 groups exhibited a significant shortening of the wound length (orange dashed vertical line), significant regeneration of epidermal and dermal tissues (purple dashed line), a clear tendency toward epithelial healing, a considerable amount of neoplastic granulation tissue (black arrows), and the emergence of a capillary lumen structure (green arrows), which suggests that diabetic wounds treated in both groups were in an active proliferative stage. Notably, in the PED4 group, almost the dermis and epithelial layer were reconstructed with clear distinction, and skin appendages close to normal epithelial tissue could also be seen (Figure 5d). Therefore, adding kaempferol to the dressings in the PED4 group may improve the wound-healing environment by modulating the immune environment and inflammatory factors.

Collagen is the main ingredient of the ECM, which dynamically anchors the cellular components of the tissue.<sup>34</sup> MT staining (collagen: blue, myofibrils: red), as depicted in Figure 5d and f, indicates the arrangement and composition of these fibers. The control group had the lowest collagen content during trauma. In comparison to the control group, the gauze and PED0 groups showed a slight tendency to promote wound healing. Contrarily, the PED2 and PED4 groups exhibited a darker blue color and denser arrangement of collagen fibers than the other groups, which suggests that the



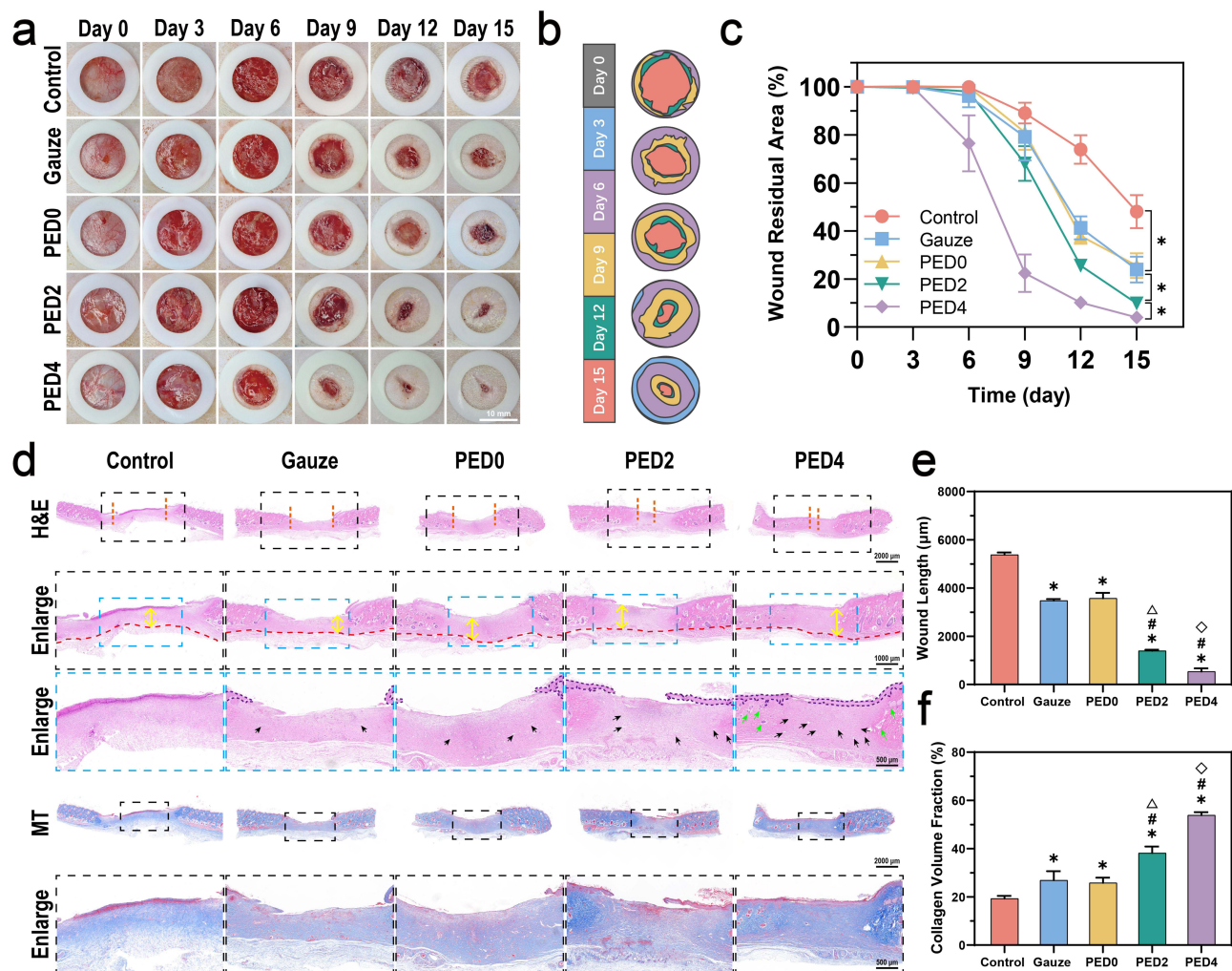


**Figure 5** Effect of varying portable electrospinning dressings on wound healing. (a) Images of wound healing over time for different dressing treatments. (b) Composite image of area changes of diabetic wound healing. (c) Analysis of residual wound area in diabetic rats ( $n = 3$ ). (d) H&E and MT staining images of wound sections. The orange dashed vertical line indicates the boundary of the wound epidermis; the red dashed line denotes the limit of the granulation tissue; the yellow arrow outlines the granulation tissue thickness; the purple dashed line represents the epidermal margin; the black arrow highlights neovascularization and the green arrow points to the skin appendages. (e) Examination of the length of diabetic wounds stained with H&E ( $n = 3$ ). (f) Assessment of collagen content of diabetic wounds using MT staining ( $n = 3$ ) (\* indicates  $p < 0.05$  compared with the control group; # indicates  $p < 0.05$  compared with PED0 group; Δ indicates  $p < 0.05$  compared with PED2 group; ◇ indicates  $p < 0.05$  compared with PED4 group).

dressing used in these groups could enhance collagen deposition. This improvement in collagen deposition may be attributed to the ability of electrospinning to mimic the ECM structure, creating a conducive environment for cell growth and facilitating collagen deposition.<sup>16</sup> Specifically, the collagen fibers in the PED4 group exhibited a greater density and a more organized arrangement, implying that kaempferol, a dressing component, might have played a role in forming a physical barrier through collagen deposition. Kaempferol potentially influenced immune cell function and suppressed inflammation, leading to the observed effects on collagen organization.<sup>35</sup>

## Evaluation of MMP9 Regulation

Studies have demonstrated that MMP9 contributes negatively to the inflammatory phase of wound healing. MMP9 upregulation is responsible for the difficulty in healing diabetic wounds in mice, making it a potential target for inflammatory therapies.<sup>6,36,37</sup> In this experiment, we found that the control group had the highest MMP9 fluorescence intensity, indicating that MMP9 was expressed in large quantities (Figure 6a and c). The gauze and PED0 groups exhibited a slight decrease in MMP9 expression, with no difference between groups. This trend aligns with the findings



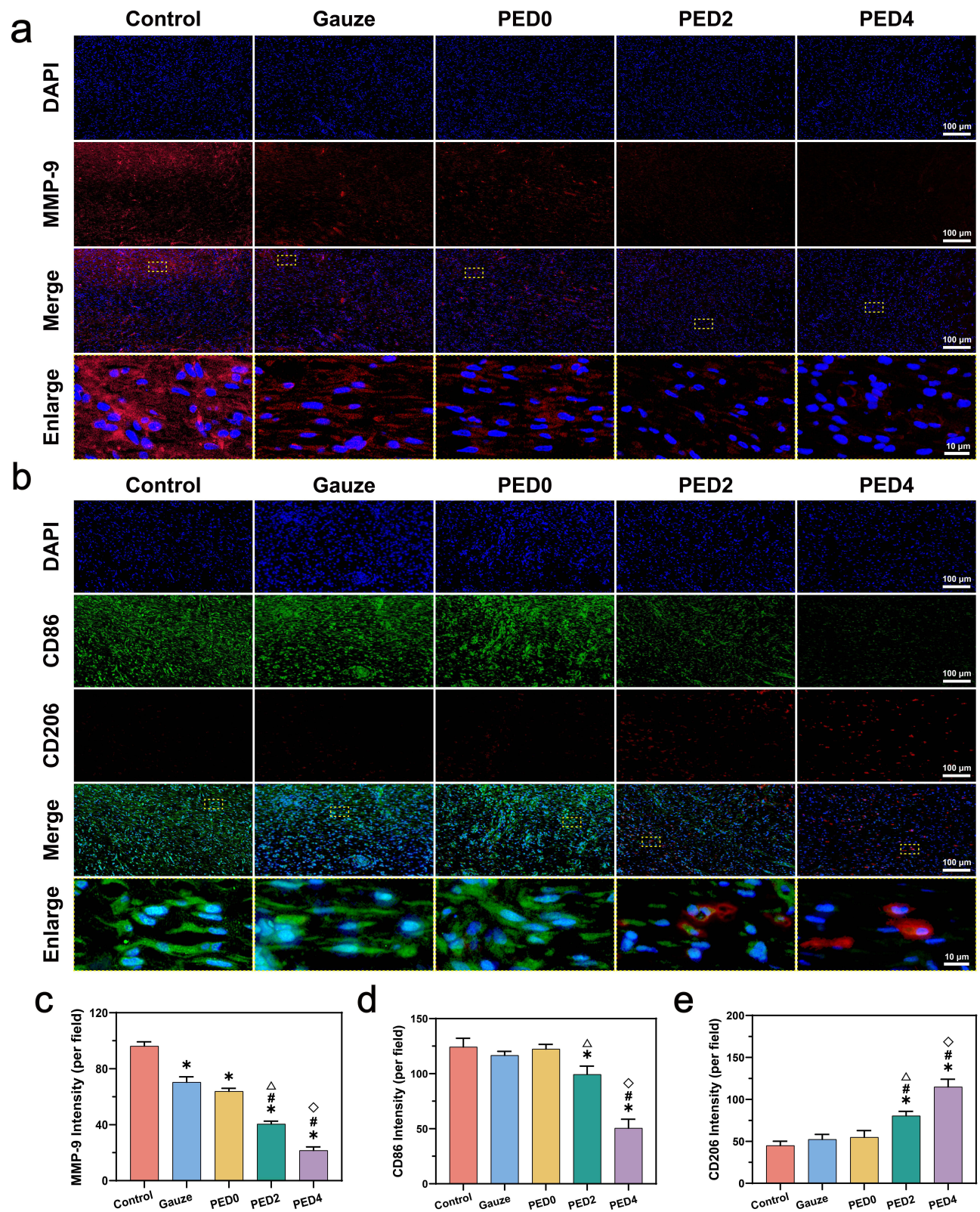


**Figure 6** Effects of various portable electrospinning dressings wound MMP9 and macrophage polarization type I diabetic rats. (a) Immunofluorescence microscopy images of MMP9 expression. (b) Immunofluorescence microscopy images of CD86 (M1 macrophage, red) expression and CD206 (M2 macrophage, green) expression. (c-e) Mean fluorescence intensity of individual fields of view for MMP9, CD86, and CD206 ( $n = 3$ ) (\* indicates  $p < 0.05$  compared with the control group; # indicates  $p < 0.05$  compared with PED0 group;  $\Delta$  indicates  $p < 0.05$  compared with PED2 group;  $\diamond$  indicates  $p < 0.05$  compared with PED4 group).



of the animal experiments above, indicating the significance of MMP9 in regulating wound healing. The mean fluorescence intensity declined in the PED2 and PED4 groups, with the lowest intensity observed in the PED4 group (Figure 6a). This suggests that kaempferol effectively suppressed the expression of MMP9, while PF-127 may have influenced the mechanical strength of the dressings, also inhibiting the expression of MMP9.<sup>38</sup> Furthermore, the SEM results of PED indicated that PF-127 altered the surface morphology of PED2 and PED4, which may also affect protein expression.<sup>39</sup> This result was also in line with the previous results of HE and MT staining, and the PED4 group presented the best wound healing trend and status. These results imply that kaempferol may suppress the NF- $\kappa$ B signaling pathway, leading to MMP9 downregulation, thereby mitigating inflammation and promoting avoidance of the apoptosis pathway.<sup>28,40</sup> Additionally, the study indicates that the combination of kaempferol and electrospinning material displays remarkable compatibility, with the electrospinning dressing serving as an effective vehicle for the wound-healing properties of kaempferol.

## Evaluation of Immune and Inflammation Regulation

M1 phenotypic macrophages play a critical role in the initial inflammatory stage of wound healing by protecting the wound from pathogens. As wound healing progresses, macrophage activation into the M2 phenotype becomes crucial in

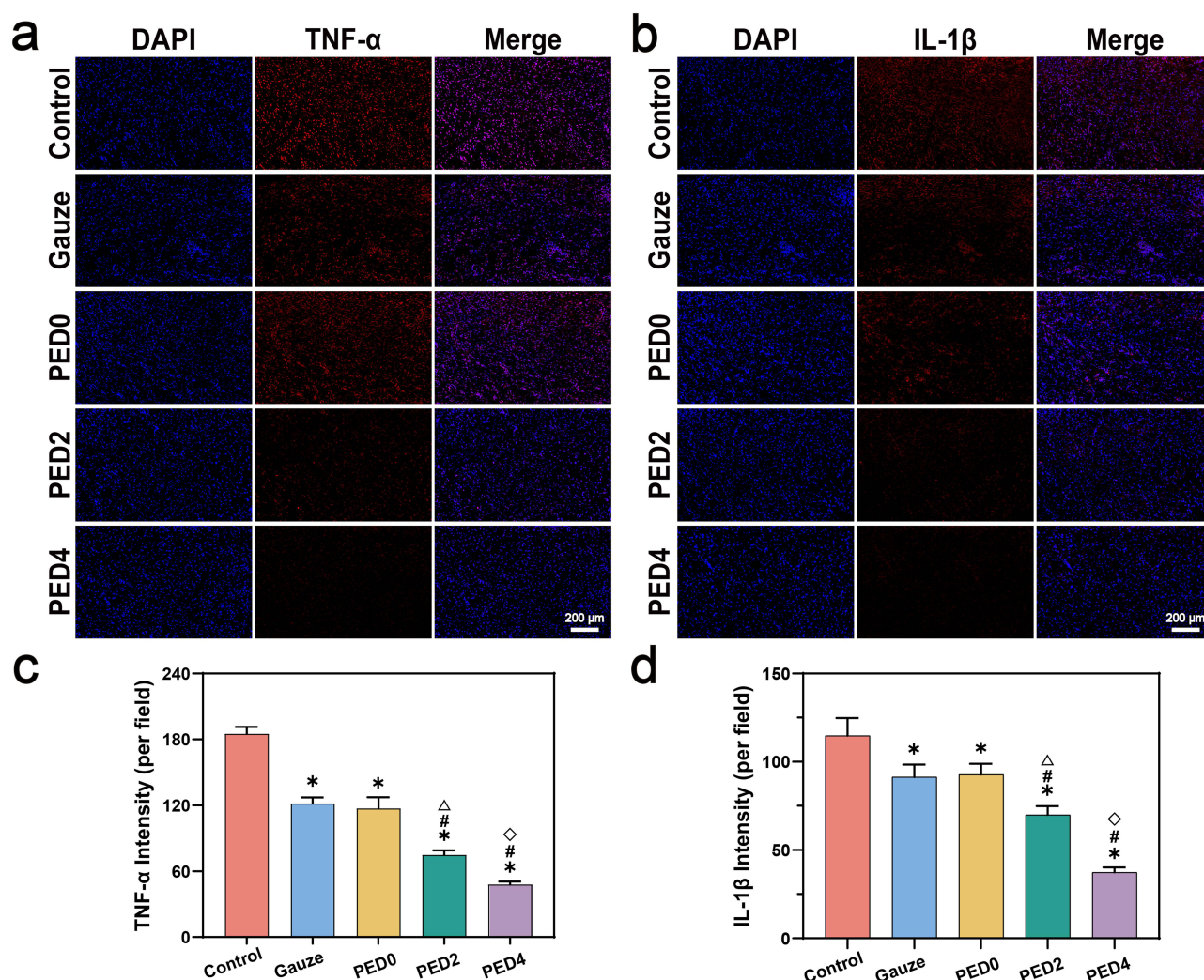


**Figure 7** Effect of portable electrospinning dressings on wound inflammatory factors in type I diabetic rats. (a-b) Immunofluorescence microscopy images of TNF- $\alpha$  and IL-1 $\beta$ . (c-d) Mean fluorescence intensity of individual fields of view for TNF- $\alpha$  and IL-1 $\beta$  ( $n = 3$ ) (\* indicates  $p < 0.05$  compared with the control group; # indicates  $p < 0.05$  compared with PED0 group;  $\Delta$  indicates  $p < 0.05$  compared with PED2 group;  $\diamond$  indicates  $p < 0.05$  compared with PED4 group).



accelerating the end of the inflammatory phase and promoting cell proliferation, angiogenesis, and inflammatory factor levels. This study assessed the polarization of macrophages in different treatment groups using CD86 and CD206 immunofluorescence staining (Figure 6b, d and e). Both PED2 and PED4 groups showed decreased CD86 fluorescence and increased CD206 fluorescence. Remarkably, in the PED4 group, the trend of transition of M1 to M2 phenotype was the most pronounced, which is consistent with the results of staining analyses of H&E, MT, and MMP9, suggesting that the high porosity of the electrospun materials and MMP9 inhibition jointly regulated the phenotypic shift of macrophages.<sup>14,36</sup> Meanwhile, the PED4 group's good vapor permeability properties loaded with 1% kaempferol played a synergistic effect in inhibiting interferon- $\gamma$ -dependent immune metabolic pathways to improve the local immune regulatory function, promoting the transition of most M1 to M2 phenotypes, and maintaining immune microenvironmental homeostasis.<sup>27,33,41</sup>

During the inflammatory phase in diabetic wounds, impaired immune regulatory mechanisms, such as TNF- $\alpha$ , IL-1 $\beta$ , and IL-6, release excessive proinflammatory cytokines. This overabundance of cytokines initiates a robust inflammatory response, which hinders the normal wound healing.<sup>42</sup> As depicted in Figure 7, 8a and c, the control, gauze, and PED0 groups had higher release of proinflammatory factors, suggesting that excessive proinflammatory factors still existed around the wounds, which is unfavorable for diabetic wound healing in rats. However, the treatment with PED2 and

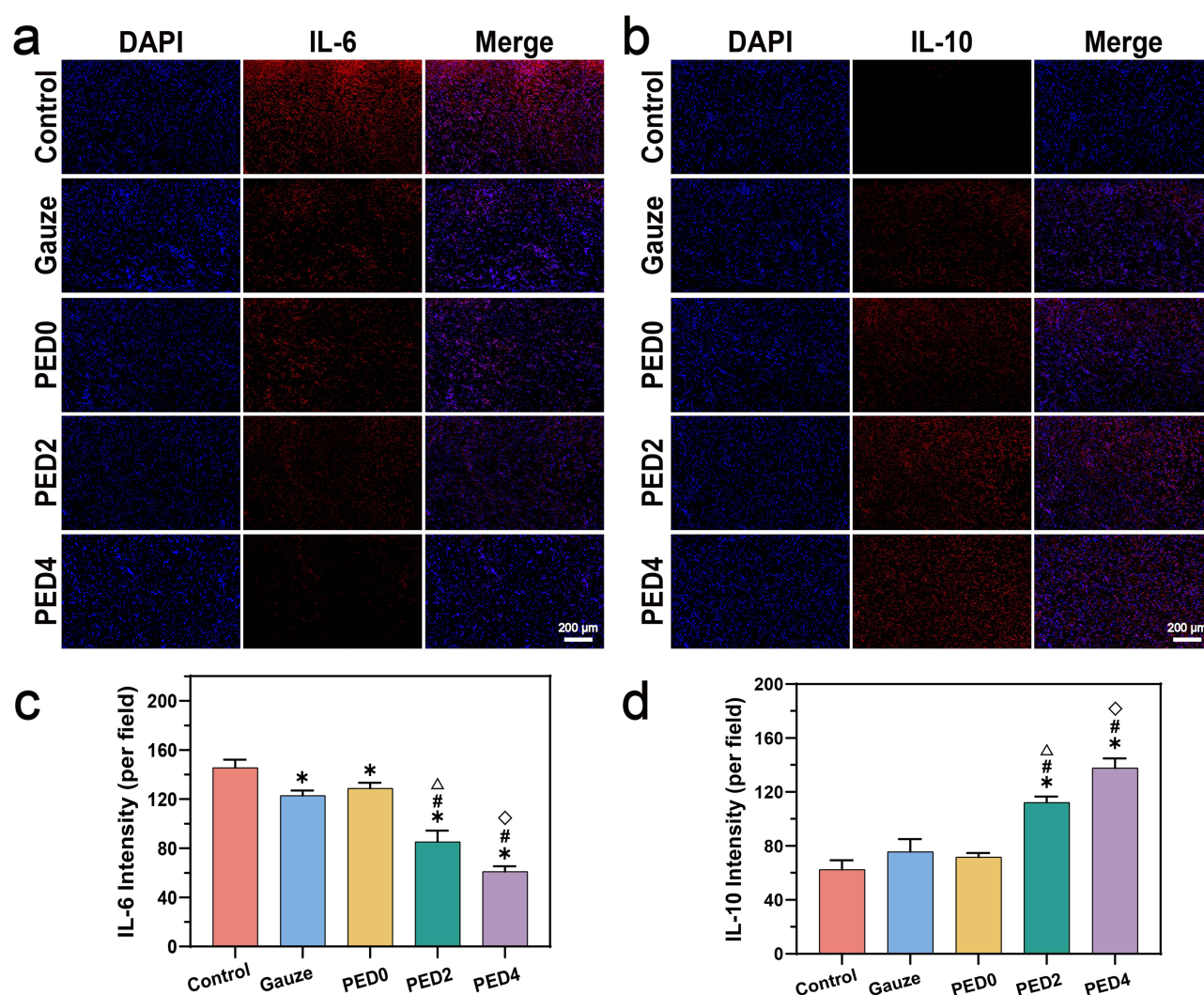


**Figure 8** Effect of portable electrospinning dressings on wound inflammatory factors in type I diabetic rats. (a-b) Immunofluorescence microscopy images of IL-6 and IL-10 expression. (c-d) Mean fluorescence intensity of individual fields of view for IL-6 and IL-10 ( $n = 3$ ) (\* indicates  $P < 0.05$  compared with the control group; # indicates  $P < 0.05$  compared with PED0 group;  $\Delta$  indicates  $P < 0.05$  compared with PED2 group;  $\diamond$  indicates  $P < 0.05$  compared with PED4 group).



PED4 dressings led to an obvious decrease in the fluorescence intensities of TNF- $\alpha$ , IL-1 $\beta$ , and IL-6. Consistent with prior research, kaempferol has been repeatedly demonstrated to engage in stable molecular interactions with MMP9.<sup>43,44</sup> Therefore, The PED4 group illustrated the most significant changes, consistent with the previous results of MMP9 regulation, indicating that kaempferol inhibits MMP9 expression and exerts an anti-inflammatory effect by decreasing anti-inflammatory factor expression.

Anti-inflammatory factors are also essential to inflammatory regulation, such as IL-10, which contributes to wound healing. In both the PED2 and PED4 groups, the IL-10 fluorescence intensity was lower than the control, gauze, and PED0 groups, indicating excellent regulation of anti-inflammatory factors (Figure 8b and d). The lowest release of IL-10 was found in the group treated with kaempferol. The combination of electrospinning with kaempferol has been demonstrated to control inflammation to a certain extent, improve the local microenvironment, and accelerate wound healing.

## Neovascularization Evaluation

Neovascularization is key to diabetic wound repair and plays a critical role in wound healing by promoting cellular immune migration, increasing nutrient and oxygen supply, and regulating scar formation.<sup>45,46</sup> VEGF and CD31 are common markers of endothelial cells indicative of neointimal formation. Compared with the control, gauze, and PED0 groups, VEGF and CD31 fluorescence intensities were significantly enhanced in the PED2 and PED4 groups (Figure 9). It may be related to the longer inflammatory period and immune disorders in diabetic wounds, as well as the persistent

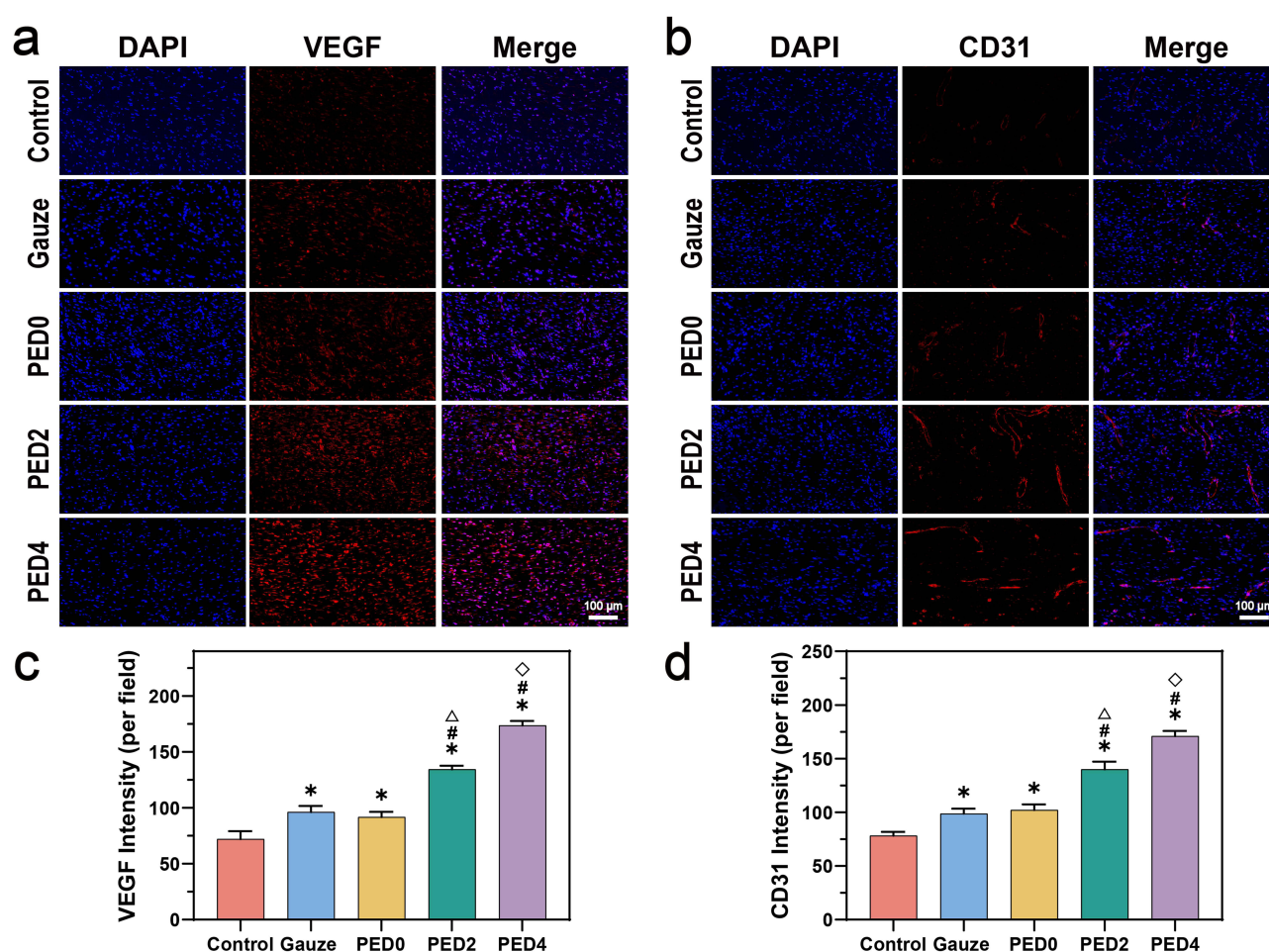


**Figure 9** Effect of portable electrospun dressings on wound neovascularization in type I diabetic rats. (a-b) Immunofluorescence microscopy images of VEGF and CD31 expression. (c-d) Mean fluorescence intensity of individual fields of view for VEGF and CD31 (n=3) (\* indicates  $p < 0.05$  compared with the control group; # indicates  $p < 0.05$  compared with PED0 group;  $\Delta$  indicates  $p < 0.05$  compared with PED2 group;  $\diamond$  indicates  $p < 0.05$  compared with PED4 group).



elevation of pro-inflammatory factors in the first three groups. Furthermore, the vapor permeability properties of PED2 and PED4 dressings promoted the neovascularization of wounds in both groups, improving the local microenvironment and resulting in a shorter time to enter the proliferative phase of the diabetic wounds. The PED4 group containing kaempferol had the most pronounced angiogenesis, and the number of official lumens and structural morphology was more pronounced, indicating that the blood supply to the wounds was superior to that of the other groups, suggesting that kaempferol was more effective in ameliorating inflammation and promoting neointimal formation and fusion. Thus, PED4 effectively corrects imbalances in wound immunomodulation, reduces inflammation, and promotes neovascularization and collagen deposition, ultimately leading to optimal DFU healing.

## Conclusion

In conclusion, the combination of kaempferol and portable electrospinning resulted in the development of a novel electrospinning fiber, PED4, which exhibited immunomodulatory effects and quickly conformed to the shape of the wound within minutes. PED4 depicted excellent vapor permeability properties, effectively regulating water evaporation from wounds while ensuring breathability. In vitro compatibility experiments demonstrated the good biocompatibility of gauze, PED0, PED2, and PED4. Furthermore, in vivo wound healing experiments in diabetic rats confirmed that PED4 promoted wound healing by enhancing skin appendage formation, collagen deposition, and extracellular matrix remodeling. Immunofluorescence assessment revealed the synergistic effects of PED4 vapor permeability and the anti-inflammatory and immunomodulatory properties of kaempferol. This led to the inhibition of MMP9, M2 macrophage polarization, improvement of the local inflammatory microenvironment by downregulating proinflammatory cytokines (TNF- $\alpha$ , IL-1 $\beta$ , and IL-6), upregulation of anti-inflammatory cytokines (IL-10), and facilitation of neovascularization regeneration, resulting in improved healing of diabetic wounds. However, portable electrospinning is limited by the choice of materials. In the future, the diversity of materials needs to be further explored and improved. In summary, this innovative approach combining natural extracts with portable electrospinning has significant implications for enhancing the management of chronic wounds in clinical practice.

## Ethics Approval and Consent

The use of experimental animals in this study has been approved by the Institutional Animal Care and Use Committee of Jilin University. All procedures strictly adhere to the guidelines for the care and utilization of experimental animals set forth by Jilin University.

## Acknowledgments

Jianwen Li and Hongqi Meng contributed equally to this article and are both first authors. This research received financial support from the Young Scientists Fund of the National Natural Science Foundation of China under Grant/Award Number 82402917.

## Disclosure

The authors declare no conflicts of interest in this work.

## References

- McDermott K, Fang M, Boulton AJM, Selvin E, Hicks CW. Etiology, epidemiology, and disparities in the burden of diabetic foot ulcers. *Diabetes Care*. 2023;46(1):209–221. doi:10.2337/dci22-0043
- Armstrong DG, Tan TW, Boulton AJM, Bus SA. Diabetic foot ulcers: a review. *JAMA*. 2023;330(1):62–75. doi:10.1001/jama.2023.10578
- Rice JB, Desai U, Cummings AK, Birnbaum HG, Skornicki M, Parsons NB. Burden of diabetic foot ulcers for medicare and private insurers. *Diabetes Care*. 2014;37(3):651–658. doi:10.2337/dc13-2176
- Theocharidis G, Thomas BE, Sarkar D, et al. Single cell transcriptomic landscape of diabetic foot ulcers. *Nat Commun*. 2022;13(1):181. doi:10.1038/s41467-021-27801-8
- Wynn TA, Vannella KM. Macrophages in Tissue Repair, Regeneration, and Fibrosis. *Immunity*. 2016;44(3):450–462. doi:10.1016/j.immuni.2016.02.015



6. Nguyen TT, Ding DR, Wolter WR, et al. Validation of Matrix Metalloproteinase-9 (MMP-9) as a novel target for treatment of diabetic foot ulcers in humans and discovery of a potent and selective small-molecule mmp-9 inhibitor that accelerates healing. *J Med Chem.* **2018**;61(19):8825–8837. doi:10.1021/acs.jmedchem.8b01005
7. Chang M, Nguyen TT. Strategy for treatment of infected diabetic foot ulcers. *Acc Chem Res.* **2021**;54(5):1080–1093. doi:10.1021/acs.accounts.0c00864
8. Raziyeve K, Kim Y, Zharkinbekov Z, Kassymbek K, Jimi S, Saparov A. Immunology of acute and chronic wound healing. *Biomolecules.* **2021**;11(5):700. doi:10.3390/biom11050700
9. Zhou LB, Liu F, You JY, et al. A novel self-pumping janus dressing for promoting wound immunomodulation and diabetic wound healing. *Adv Healthcare Mater.* **2024**;13(10). doi:10.1002/adhm.202303460
10. Vazquez-Ayala L, Del Ángel-Olarte C, Escobar-García DM, et al. Chitosan sponges loaded with metformin and microalgae as dressing for wound healing: a study in diabetic bio-models. *Int J Biol Macromol.* **2024**;254(Pt 1):127691. doi:10.1016/j.ijbiomac.2023.127691
11. Qi X, Cai E, Xiang Y, et al. An immunomodulatory hydrogel by hyperthermia-assisted self-cascade glucose depletion and ROS scavenging for diabetic foot ulcer wound therapeutics. *Adv Mater.* **2023**;35(48):e2306632. doi:10.1002/adma.202306632
12. Zhu S, Zhao B, Li M, et al. Microenvironment responsive nanocomposite hydrogel with NIR photothermal therapy, vascularization and anti-inflammation for diabetic infected wound healing. *Bioact Mater.* **2023**;26:306–320. doi:10.1016/j.bioactmat.2023.03.005
13. Abdelgawad AM, Hudson SM, Rojas OJ. Antimicrobial wound dressing nanofiber mats from multicomponent (chitosan/silver-NPs/polyvinyl alcohol) systems. *Carbohydr Polym.* **2014**;100:166–178. doi:10.1016/j.carbpol.2012.12.043
14. Yu J, Lin Y, Wang G, et al. Zein-induced immune response and modulation by size, pore structure and drug-loading: application for sciatic nerve regeneration. *Acta Biomater.* **2022**;140:289–301. doi:10.1016/j.actbio.2021.11.035
15. Yan X, Yu M, Ramakrishna S, Russell SJ, Long YZ. Advances in portable electrospinning devices for delivery of personalized wound care. *Nanoscale.* **2019**;11(41):19166–19178. doi:10.1039/c9nr02802a
16. Keirouz A, Chung M, Kwon J, Fortunato G, Radaesi N. 2D and 3D electrospinning technologies for the fabrication of nanofibrous scaffolds for skin tissue engineering: a review. *Wiley Interdiscip Rev Nanomed Nanobiotechnol.* **2020**;12(4):e1626. doi:10.1002/wnan.1626
17. Brown TD, Daltona PD, Hutmacher DW. Melt electrospinning today: an opportune time for an emerging polymer process. *Prog Polym Sci.* **2016**;56:116–166. doi:10.1016/j.progpolymsci.2016.01.001
18. Zhang D, Xu D, Huang X, et al. Puerarin-loaded electrospun patches with anti-inflammatory and pro-collagen synthesis properties for pelvic floor reconstruction. *Adv Sci.* **2024**;11(21):e2308590. doi:10.1002/adv.202308590
19. Zhou LB, Hu Z, Liu F, et al. Electrospun Self-Pumping dressing with gastrodin for immunomodulation and rapid healing of diabetic wounds. *Article Chem Eng J.* **2024**;495:153424. doi:10.1016/j.cej.2024.153424.
20. Yue Y, Gong X, Jiao W, et al. In-situ electrospinning of thymol-loaded polyurethane fibrous membranes for waterproof, breathable, and antibacterial wound dressing application. *J Colloid Interface Sci.* **2021**;592:310–318. doi:10.1016/j.jcis.2021.02.048
21. Zhao YT, Zhang J, Gao Y, et al. Self-powered portable melt electrospinning for in situ wound dressing. *J Nanobiotechnol.* **2020**;18(1):111. doi:10.1186/s12951-020-00671-w
22. Calderón-Montaña JM, Burgos-Morón E, Pérez-Guerrero C, López-Lázaro M. A review on the dietary flavonoid kaempferol. *Mini-Rev Med Chem.* **2011**;11(4):298–344. doi:10.2174/138955711795305335
23. Chen AY, Chen YC. A review of the dietary flavonoid, kaempferol on human health and cancer chemoprevention. *Food Chem.* **2013**;138(4):2099–2107. doi:10.1016/j.foodchem.2012.11.139
24. Yang L, Gao YC, Bajpai VK, et al. Advance toward isolation, extraction, metabolism and health benefits of kaempferol, a major dietary flavonoid with future perspectives. *Crit Rev Food Sci Nutr.* **2023**;63(16):2773–2789. doi:10.1080/10408398.2021.1980762
25. Ju PC, Ho YC, Chen PN, et al. Kaempferol inhibits the cell migration of human hepatocellular carcinoma cells by suppressing MMP-9 and Akt signaling. *Environ Toxicol: Int J.* **2021**;36(10):1981–1989. doi:10.1002/tox.23316
26. Li CL, Zhao YW, Yang D, et al. Inhibitory effects of kaempferol on the invasion of human breast carcinoma cells by downregulating the expression and activity of matrix metalloproteinase-9. *Biochem Cell Biol.* **2015**;93(1):16–27. doi:10.1139/bcb-2014-0067
27. Zhao JN, Ling LB, Zhu W, et al. M1/M2 re-polarization of kaempferol biomimetic NPs in anti-inflammatory therapy of atherosclerosis. *J Control Release.* **2023**;353:1068–1083. doi:10.1016/j.jconrel.2022.12.041
28. Liu Z, Yao X, Sun B, et al. Pretreatment with kaempferol attenuates microglia-mediate neuroinflammation by inhibiting MAPKs-NF-κB signaling pathway and pyroptosis after secondary spinal cord injury. *Free Radic Biol Med.* **2021**;168:142–154. doi:10.1016/j.freeradbiomed.2021.03.037
29. Wang Z, Ou X, Guan L, et al. Pomegranate-inspired multifunctional nanocomposite wound dressing for intelligent self-monitoring and promoting diabetic wound healing. *Biosens Bioelectron.* **2023**;235:115386. doi:10.1016/j.bios.2023.115386
30. Ou XL, Guan L, Guo WL, et al. Graphene oxide-based injectable conductive hydrogel dressing with immunomodulatory for chronic infected diabetic wounds. *Mater Des.* **2022**;224:ARTN111284. doi:10.1016/j.matdes.2022.111284
31. Meng WL, Lin Z, Cheng X, et al. Thiourea-cation chelation based hydrogel and its application as antibacterial dressing for the repair of diabetic wound. article; early access. *Adv Funct Mater.* **2024**;2024. doi:10.1002/adfm.202314202
32. Pathan N, Iadnut A, Tewtrakul S. Anti-inflammatory and wound healing effects of mouth gel containing kaempulchraol K from Kaempferia galanga rhizomes. *J Ethnopharmacol.* **2024**;324:117762. doi:10.1016/j.jep.2024.117762
33. Chang S, Li X, Zheng Y, et al. Kaempferol exerts a neuroprotective effect to reduce neuropathic pain through TLR4/NF-κB signaling pathway. *Phytother Res.* **2022**;36(4):1678–1691. doi:10.1002/ptr.7396
34. Huang J, Heng S, Zhang W, et al. Dermal extracellular matrix molecules in skin development, homeostasis, wound regeneration and diseases. *Semin Cell Dev Biol.* **2022**;128:137–144. doi:10.1016/j.semcdb.2022.02.027
35. Kearney KJ, Ariëns RAS, Macrae FL. The role of fibrin(ogen) in wound healing and infection control. *Semin Thromb Hemost.* **2022**;48(2):174–187. doi:10.1055/s-0041-1732467
36. Li Y, Zhang X, He D, Ma Z, Xue K, Li H. 45S5 Bioglass® works synergistically with siRNA to downregulate the expression of matrix metalloproteinase-9 in diabetic wounds. *Acta Biomater.* **2022**;145:372–389. doi:10.1016/j.actbio.2022.04.010
37. Krishnaswamy VR, Mintz D, Sagi I. Matrix metalloproteinases: the sculptors of chronic cutaneous wounds. *Biochim Biophys Acta, Mol Cell Res.* **2017**;1864(11):2220–2227. doi:10.1016/j.bbamer.2017.08.003



38. Li S, Yang C, Li J, et al. Progress in pluronic F127 derivatives for application in wound healing and repair. *Int J Nanomed*. 2023;18:4485–4505. doi:10.2147/ijn.S418534
39. Guo Y, Ao Y, Ye C, et al. Nanotopographic micro-nano forces finely tune the conformation of macrophage mechanosensitive membrane protein integrin  $\beta(2)$  to manipulate inflammatory responses. *Nano Res*. 2023;1–15. doi:10.1007/s12274-023-5550-0.
40. Lee CJ, Moon SJ, Jeong JH, et al. Kaempferol targeting on the fibroblast growth factor receptor 3-ribosomal S6 kinase 2 signaling axis prevents the development of rheumatoid arthritis. *Cell Death Dis*. 2018;9(3):401. doi:10.1038/s41419-018-0433-0
41. Hofer S, Geisler S, Lisandrelli R, et al. Pharmacological targets of kaempferol within inflammatory pathways-A hint towards the central role of tryptophan metabolism. *Antioxidants (Basel)*. 2020;9(2). doi:10.3390/antiox9020180
42. Czajka C. Capturing chemokines in chronic wounds. *Science*. 2017;356(6335):280. doi:10.1126/science.356.6335.280-b
43. Dong Q, Ren G, Li Y, Hao D. Network pharmacology analysis and experimental validation to explore the mechanism of kaempferol in the treatment of osteoporosis. *Sci Rep*. 2024;14(1):7088. doi:10.1038/s41598-024-57796-3
44. Li N, Chen S, Deng W, et al. Kaempferol attenuates gouty arthritis by regulating the balance of Th17/Treg cells and secretion of IL-17. *Inflammation*. 2023;46(5):1901–1916. doi:10.1007/s10753-023-01849-8
45. Xiong Y, Lin Z, Bu P, et al. A whole-course-repair system based on neurogenesis-angiogenesis crosstalk and macrophage reprogramming promotes diabetic wound healing. *Adv Mater*. 2023;35(19):e2212300. doi:10.1002/adma.202212300
46. He F, Xu PQ, Zhu ZK, et al. Inflammation-responsive hydrogel accelerates diabetic wound healing through immunoregulation and enhanced angiogenesis. *Adv Healthcare Mater*. 2024. doi:10.1002/adhm.202400150

## International Journal of Nanomedicine

### Publish your work in this journal

The International Journal of Nanomedicine is an international, peer-reviewed journal focusing on the application of nanotechnology in diagnostics, therapeutics, and drug delivery systems throughout the biomedical field. This journal is indexed on PubMed Central, MedLine, CAS, SciSearch®, Current Contents®/Clinical Medicine, Journal Citation Reports/Science Edition, EMBase, Scopus and the Elsevier Bibliographic databases. The manuscript management system is completely online and includes a very quick and fair peer-review system, which is all easy to use. Visit <http://www.dovepress.com/testimonials.php> to read real quotes from published authors.

Submit your manuscript here: <https://www.dovepress.com/international-journal-of-nanomedicine-journal>

**Dovepress**  
Taylor & Francis Group